Skin formation in adhesive mortars evaluated by MRI and interfacial rheology

A.L. L Fujii-Yamagata, F.A. A Cardoso, V. Sarou-Kanian, A. Daubresse, E.
Prat, Mohend Chaouche

HAL Id: hal-03070385
https://hal.science/hal-03070385

Skin formation in adhesive mortars evaluated by MRI and interfacial rheology

A. L. Fujii-Yamagata[1], F. A. Cardoso[2], V. Sarou-Kanian[3], A. Daubresse[4], E. Prat[4], M. Chaouche[1]

1 Laboratoire de Mécanique et Technologie, École Normale Supérieure Paris-Saclay/CNRS/UMR8534, Cachan, France

2 Department of Construction Engineering, Escola Politécnica, University of São Paulo, São Paulo, Brazil

3 CNRS UPR 3079 CEMHTI, Université d'Orléans, Orléans, France

4 Centre d'Innovation Parexgroup, St Quentin Fallavier, France

e-mail: alessandra.yamagata@gmail.com

Abstract

The formation of a dry skin on fresh adhesive mortars is an undesirable side effect of polymeric admixtures that are indispensable to this type of material. This investigation adapted a classical interfacial rheology technique to study the evolution of the skin's properties. The introduced technique and magnetic resonance imaging (MRI) were used to evaluate the effects of cellulose ether (CE) content and degree of substitution's (DS) on skin formation of mortars prepared with two types of cements. MRI results of water distribution within the sample over time indicated a dryer zone formed at the exposed surface that is dependent on CE content. Oscillatory interfacial measurements pointed out that skin's storage modulus (G') was firstly dominated by water loss, presenting smaller increasing rate with higher CE content, then an inversion occurred due to polymer properties predominance. Wind conditions accelerated the effects of CE on G' kinetics of the skin.

keywords: adhesive mortar, MHEC, interfacial rheology, MRI, drying

1 Introduction

Adhesive mortars consist of cement, sand, mineral fillers and a variety of additives (cellulose ethers, air-entraining, latex, etc.). They are used to glue tiles to the wall or floor substrates, including concrete, screed, plaster or render. They are usually applied to a large surface with a toothed-comb trowel that ensures the layer thickness is the same over the entire area; and forms ribs that allows excess material to squeeze out when the tile is pressed against the mortar, thus helping to promote good contact between tile and mortar along the entire interface. To obtain a suitable performance when the tile is installed, the mortar rheological properties must retain good contact, even after several minutes of exposure to ambient conditions (open time) at either internal or external building areas. For this purpose, additives are often used to obtain these properties.

Cellulose ether-based admixtures (CEs) are one of the main additives used in adhesive mortar due to their thickening effect and their water retaining ability, which is important for fresh mortar properties [1,2]. However, CEs can also generate an undesirable side effect of skin formation [3,4]. The skin is a surface layer with different properties compared to the bulk body underneath [5] and, in adhesive mortars, is

formed due to water drying from the surface layer. It is also related to film formation and carbonation [2,4]. Zurbriggen et al. [6] defines skin as a 0.1 mm thin layer at the surface and crust as a dry thicker layer of about 1 mm after 30 min of exposure, in this investigation skin will be defined as the air-mortar interface which englobes both thin skin layer and crust, since in the rheological point of view we cannot distinguish both. The dry external layer (skin) at the mortar-air interface should be avoided because it may be difficult to be removed during tile emplacement and it can hinder the mortar capability to wet the tile surface properly [4,5]. This last effect is assessed by the industry through the standard EN1347 – determination of wetting capability. The procedure states that the mortar is applied on a standard concrete substrate and after different waiting times (10, 20 and 30 minutes) a glass tile (10cm x 10cm) is placed over the mortar and squeezed for 30 s with a 50±0.5 N weight. The wetting ability of the fresh mortar is expressed by the area of contact between the mortar and glass tile, and the result is indicated as a percentage of the plate's total area (e.g. through planimetrics) [7]. This test, however, fails to identify dry contact areas between mortar and tile that result in low adhesion [5].

Recent studies have been trying to improve existing methods and characterize skin formation in detail. Zurbriggen et al. [8] suggested a modification of EN1347 that included a shallow angle illumination of the mortar-glass contact, which allows for the observation of unwetted areas. Even though this technique can improve the standard method and provide more precise evaluation of the contact, the interfacial properties are not directly assessed. Bühler et al. [5] investigated the chemical composition, microstructure and physical properties of adhesive mortar's skin. They concluded that skin formation can be explained by the drying of the mortar surface and related mechanisms of organic and inorganic films formation composed of cellulose ether (CE), polymers, carbonates and minor hydrates. Póvoas [9] studied skin formation through a tack test, Diffuse Reflectance Infrared Fourier Transform spectrometry (DRIFT) and environmental Scanning Electron Microscopy (SEM), and showed that after re-humidification of the mortars surface, skin was dissolved and adhesion was recovered, except for the cases in which drying was intense and a more stable skin formed. Póvoas [9] have also identified the formation of latex film with hydroxyl ethyl cellulose (HEC) and evidence of a discontinuous film without HEC. Jenni et al. [4] used Fluorescence laser scanning microscopy (LSM) to follow Latex, CE and PVA mobility inside the mortar. In this investigation, the authors observed that evaporation induced water flux to the surface and capillary forces pulled water to the porous substrate. The migration of pore water led to fractionation of dissolved species, resulting in distinct enrichment of PVA and CE above the substrate. They concluded from studies on failure surfaces that mortar-tile represents the weakest part in the system, and, in this context, skinning reduces adhesive strength [4]. Skin formation have an import role on adhesion, therefore, research and further developments should focus on improvement of techniques to its characterization.

The wide surface area in which material is applied (substrate-mortar interface) and exposed to (air-mortar interface) before tile placement generates a great loss of water that not only has an intrinsic influence on the mortar's properties [10], but also affects skin formation. As the initial contact between fresh mortar and tile is the first step for the development of interfacial microstructure, for the adhesive properties between the materials, the comprehension of the rheological behavior at the air-mortar interface and its evolution with time and drying is of great importance for mortar producers and users. To date, different studies have focused on the bulk rheological properties of adhesive mortars or pastes [11–13]; however, direct rheological measurements of the skin are still very limited. Petit et al. [14] adapted a food protocol for "solid" samples [15], making punctual shear measurement with a plate-plate geometry of a sample after 20 and 30 minutes of exposure, where a skin formed. Zurbriggen et al. [16] evaluated the crust rigidity by a needle-penetration method where a needle is inserted at a constant velocity in the mortar while the normal force (mN) is obtained, it delivers rheological profiles from the surface downwards. By repeating such measurement at laterally different locations of the same mortar sample one can follow the

dynamic build-up of a crust layer [16]. In domains like biochemical, chemical, pharmaceutical, food and petroleum, interfacial rheology is widely used [17–20]. In these areas, the characterization of different types of emulsions and their stability is crucial [21,22] and diverse interfacial methods are used, such as oscillation drop, bi-cone, double wall ring and double wall ring for shear properties [18,19].

Current interfacial rheological techniques are not suitable to measure granular materials such as mortar. Granular materials require a technique that reduces bulk effects and is able to measure materials with high viscosity that contain mm-range particles. Another requirement is to avoid slip effects that are critical for concentrated suspensions. Therefore, the objective of this paper is to investigate skin formation of adhesive mortars. Firstly, MRI is used to assess water distribution within the specimen during the first fresh hours and to determine skin layer depth as well. Then, an interfacial rheology technique, inspired by classical methods, is introduced to evaluate skin properties. The effects of cellulose ether (CE) content and type on bulk and interfacial rheological properties of adhesive mortars with gray and white cements is evaluated through oscillatory rheometry. Different environmental conditions are also employed to evaluate the effect of wind on skin formation.

2 Experimental

2.1 Experimental plan

The structure of this investigation is shown in Table 1. MRI and rheological techniques evaluated adhesive mortar formulations with variations of cement type and of cellulose ether (CE) type and content. Environmental condition was also modified to evaluate skin formation.

Table 1. Scheme of variables of adhesive mortar formulations and tests carried in this investigation

Formulations			Tests
	CE Type	**CE Content**	
white cement	CE-A	0.1%	MRI Bulk rheology Interfacial rheology Evaporation
		0.25%	
		0.4%	
	CE-B	0.25%	Bulk rheology Interfacial rheology Evaporation
	CE-C	0.25%	
gray cement	CE-A	0.1%	Bulk rheology (*only) Interfacial rheology (with and without wind) Evaporation
		0.2%*	
		0.25%	
		0.3%*	
		0.4%	
		0.5*	
	CE-B	0.25%	Bulk rheology Interfacial rheology Evaporation
	CE-C	0.25%	

2.2 Materials

2.2.1 Cement and sand

This work employed basic compositions of adhesive mortars and two types of cements: white CEM I 52,5 N CE CP2 NF and gray CEM I 52,5 N CE CP2 NF, both from Lafarge. Cement phases, density, and blaine fineness obtained with the manufacturer are shown in Table 2.

Table 2. Phase compositions, density and blaine fineness of the investigated cements

Phase	white CEM I	gray CEM I
C_3S (wt%)	58	61
C_2S (wt%)	28	14.3
C_3A (wt%)	6	12
C_4AF (wt%)	1	7.9
Gypsum (wt%)	5	4.6
Density (g/cm^3)	3.08	3.14
Blaine fineness (cm^2/g)	4250	3519

The sand used in this study was a silica sand PE2LS from FULCHIRON. ASTM granulometric distribution from the manufacturer is shown in Figure 1.
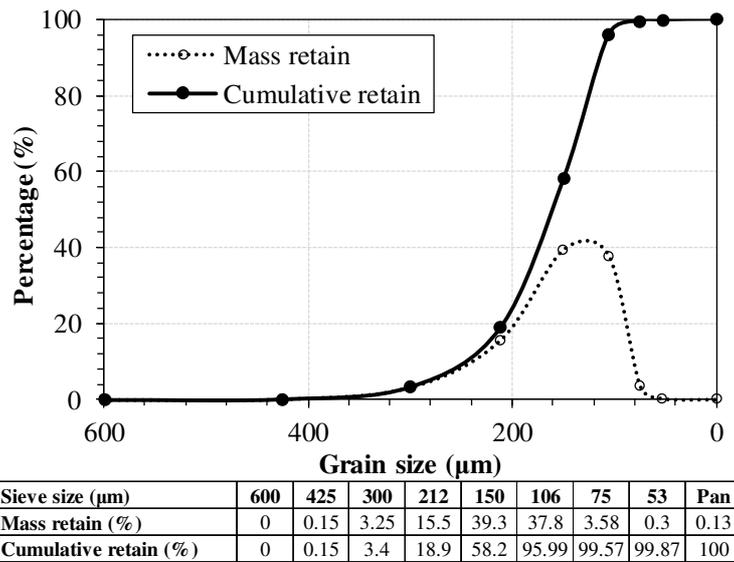

Sieve size (µm)	600	425	300	212	150	106	75	53	Pan
Mass retain (%)	0	0.15	3.25	15.5	39.3	37.8	3.58	0.3	0.13
Cumulative retain (%)	0	0.15	3.4	18.9	58.2	95.99	99.57	99.87	100

Figure 1. Granulometric distribution of sand used in this investigation obtained from the manufacturer.

2.2.2 Cellulose ethers

Cellulose ethers (CEs) are additives used in mortars as thickening and water retaining agents [24]. Due to their surfactant behavior, they also influence air entrainment and air-void stabilization. The addition of CE is important in adhesive mortars to improve workability, guarantee stickiness, and extend open time. Higher air-entrainment and bubble stabilization can improve workability and efficiency. Its thickening effect improves tackiness and stickiness, so the tile and the substrate are well attached during the fresh state [25]. A water retaining effect is important to maintain enough water for hydration and allow longer open time.

CEs are water-soluble polymers with a high molecular weight derived from cellulose (consisting of a long chain of repeating anhydroglucose units) through replacement of a certain fraction of the hydroxyl groups by hydroxy-alkyl groups. These form different CEs: HydroxyPropyl Cellulose (HPC), HydroxyPropyl Methyl Cellulose (HPMC/MHPC), Hydroxyl Ethyl Methyl Cellulose (HEMC/MHEC), etc. Fundamentally, the substitution process allows for transforming water-insoluble cellulose into a water-soluble polymer, which can then be easily dispersed in various industrial products that comprise an aqueous phase [3,26]. The CEs mode of action can be classified in different categories [27]:

(1) Adsorption. The long-chain polymer molecules adhere to the periphery of water molecules, thus adsorbing, fixing part of the kneading water, and thereby expanding. This increases the viscosity of the mix water and that of the cement-based product [27]. Three types of water in hydrated polymers have been classified: free water (TypeI), freezing bound water (TypeII), and nonfreezing bound (TypeIII). The sum of freezing and nonfreezing bounds is called the bound water, which is strongly associated with the hydrophilic groups of a polymer. It shows different molecules distribution and repeating structure compared to free water and vary depending on the substitution type of polymer [28].

(2) Association. Molecules in adjacent polymer chains can develop attractive forces, thus further blocking the motion of water, causing a gel formation and an increase in viscosity.

(3) Intertwining. At low rates of shear, and especially at high concentrations, the polymer chains can intertwine and entangle, resulting in an increase in the apparent viscosity. Such entanglement can disaggregate, and the polymer chains can align in the direction of the flow at high shear rates, resulting in shear thinning.

(4) Crystallization. Hydrophobic associations of the molecules can generate the formation of fringe micelles and compact crystal in certain conditions that can play a role on the solution viscosity and the enhancement of its viscoelasticity [29,30].

The CEs considered in this research were of the hydroxyethyl methyl cellulose type (MHEC). The CE samples were provided by Dow Chemical Company and used as they were received. They varied in the following parameters: viscosity, molar substitution ratio (MS), and degree of substitution (DS). These parameters were provided by the manufacturer and are shown in Table 3. The viscosity corresponds to that of a 2% by weight aqueous polymer solution, as measured with a Brookfield RV viscometer at 20 rpm. The value of the viscosity gives an indication of the average molecular weight of the polymer. Yet, the interstitial solution in mortar matrix presents a different pH and ionic strength that may affect the polymer interactions and, as result, may affect the final viscosity that would be obtained [3].

Table 3. Properties of the cellulose ethers used in this investigation, as provided by the manufacturer.

Labels in text	Viscosity (mPa.s)	MS	DS
CE-A	40000	0.2-0.25	1.62-1.65
CE-B	40000	0.1-0.2	1.8-1.9
CE-C	40000	0.2	1.4

2.2.3 Mix design

Common formulations of adhesive mortars were used (Table 4). They contained white or gray Portland cement, silica sand, an organic binder in redispersible powder form (latex: vinyl acetate, vinyl versatate and a maleic ester copolymer resin) and an organic modifier (CE: hydroxyethyl methyl cellulose). Different contents of CE (CE-A) were used and three different CEs with varying degree of substitution were also employed (CE-A, CE-B, CE-C). No formulation with less than 0.1% of CE was used to avoid

significant phase separation. The formulations codes in Table 4 are defined to its content: "w" or "g" refers to white or gray cement; the percentage is the CE content; and "A," "B," or "C" refers to the type of polymer.

Table 4. Formulations of adhesive mortars with white and gray cement, with different cellulose ether content and type (wt%)

Formulations	Gray CEM I	White CEM I	Sand	Latex	CE-A	CE-B	CE-C	Water/ powder	Entrained air
w_0.1% CE-A	-	30%	67.40%	2.5%	0.1%	-	-		14%
w_0.25% CE-A	-	30%	67.25%	2.5%	0.25%	-	-		19%
w_0.4% CE-A	-	30%	67.10%	2.5%	0.4%	-	-		21%
w_0.25% CE-B	-	30%	67.25%	2.5%	-	0.25%	-		20%
w_0.25% CE-C	-	30%	67.25%	2.5%	-	-	0.25%		19%
g_0.1% CE-A	30%	-	67.40%	2.5%	0.1%	-	-		13%
g_0.2% CE-A	30%	-	67.30%	2.5%	0.2%	-	-	0.205	20%
g_0.25% CE-A	30%	-	67.25%	2.5%	0.25%	-	-		20%
g_0.3% CE-A	30%	-	67.20%	2.5%	0.3%	-	-		22%
g_0.4% CE-A	30%	-	67.10%	2.5%	0.4%	-	-		22%
g_0.5% CE-A	30%	-	67.00%	2.5%	0.5%	-	-		22%
g_0.25% CE-B	30%	-	67.25%	2.5%	-	0.25%	-		19%
g_0.25% CE-C	30%	-	67.25%	2.5%	-	-	0.25%		18%

2.3 Methods

2.3.1 Magnetic Resonance Imaging (MRI)

Due to MRI's ability to identify water content and form inside a sample, it is a powerful technique for cementitious materials in which water has a main role regarding agglomeration, rheological behavior, hydration and microstructural development. Recent studies have been exploring the technique as Fourmentin et al. [31] that evaluated the liquid transfer between a cement paste and a porous media with nuclear magnetic resonance (NMR). Faiyas et al. [32] evaluated moisture distribution and hydration characteristics of adhesive mortars with MRI and NMR. Jarny et al. [33] even combined rheological measurements and MRI technique simultaneously, hence following cement paste liquid to solid transition. This research contributes to the previously mentioned research by combining the use of MRI with interfacial rheology technique.

MRI is based upon the interaction between a magnetic field and nuclei that possesses a spin angular momentum. Every periodic table element, except argon and cerium, has at least one isotope that possesses this angular momentum. A nucleus containing an odd number of protons or neutrons has a characteristic motion or precession. Nuclei are charged particles, so their precession produces a small magnetic moment that can interact with an external magnetic field. [1]H is one of the most abundant isotopes for hydrogen and its response to an applied magnetic field is one of the largest found in nature [34]. Thus, hydrogen is a natural choice for MRI measurements. When a sample is placed in a large magnetic field, many of the free hydrogen nuclei align themselves with the direction of the magnetic field. The nuclei precess about the magnetic field direction, which is known as Larmor precession behavior. The frequency of Larmor precession is proportional to the applied magnetic field strength, as defined by Larmor frequency, ω_0:

$$\omega_0 = \gamma B_0. \tag{1}$$

The technique is based on the gyromagnetic ratio, and γ is the strength of the applied magnetic field. The gyromagnetic ratio is a nuclei specific constant. For hydrogen, $\gamma = 42.58\ MHz.T^{-1}$.

To obtain an MR image of an object, the object is placed in a uniform magnetic field, B_0. As a result, the object's hydrogen nuclei align with the magnetic field and create a net magnetic moment, M, parallel to B_0. Then, a radio-frequency (RF) pulse, B, is applied perpendicular to B_0. This pulse, with a frequency equal to the Larmor frequency, causes M to tilt away from a proton spin excitation followed by signal acquisition of the spin-spin relaxation. Once the RF signal is removed, the nuclei realign themselves such that their net magnetic moment, M, is again parallel with B_0. This return to equilibrium is referred to as relaxation. During relaxation, the nucleus loses energy by emitting its own RF signal. This signal is referred to as the free-induction decay (FID) response signal. The FID response signal is measured by a conductive field coil placed around the object being imaged. This measurement is processed or reconstructed to obtain MRI images [34,35].

2.3.1.1 2D MRI

To determine the layer thickness at the air-mortar interface affected by drying, the distribution of free water inside the sample was measured through magnetic resonance imaging (MRI). With spatially resolved T2 methods, a 2D distribution of free water was obtained from a section of the sample as illustrated by Figure 2a. The equipment used was a 750WB UltraStrabilized from *Bruker*. Each mortar was put in a cylindrical Teflon holder of 21 mm diameter and 7 mm height just after mixing, and then flattened with a spatula and put in the spectrometer immediately. Then, an acquisition of T2 echo was done every five minutes for two hours. The room temperature was kept at 23±1°C and 30% RU.

2.3.1.2 1D MRI

The equipment used was an Ascend 400 WB from *Bruker* with a static magnetic field of 9.4T. For the 1D distribution, the mortar was put in a glass cylindrical holder of 8 mm diameter and 4 mm height as illustrated by Figure 2b. The signal obtained was from a horizontal cut through all the sample depth. Data acquisition was done every five minutes for two hours. For 1D and 2D distribution, room temperature was kept at 23±1°C and 30% RU.
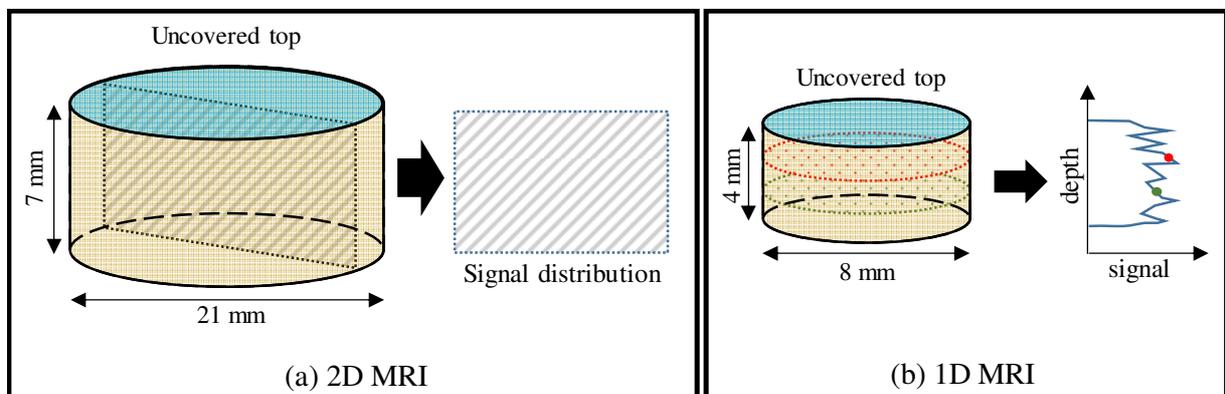

Figure 2. MRI samples scheme: (a) 2D MRI – sample dimensions and section cut of signal visualization; (b) 1D MRI – sample dimensions and representation of signal distribution obtained

2.3.2 Bulk rheology

The bulk rheological properties were evaluated through a low amplitude oscillatory technique. This consists of applying an oscillatory rotation of an amplitude small enough that it will not affect the structuring process of cement particles. From the stress response, the storage modulus (G') and loss modulus (G") are obtained. The storage modulus represents the elastic response and the loss modulus represents the viscous response, as the material changes from a viscous to a predominant elastic behavior during cement setting. Since the storage modulus is the parameter that undergoes a greater variation

during consolidation and drying, this parameter will be explored for rheological property evaluation as further explained in section 3.2.

The bulk measurements were performed with a vane geometry fully immersed in a rheometer cup as illustrated in Figure 4a. Vane geometry is a well-known geometry for granular materials that has been extensively used and investigated [36]. This has the advantage of reducing the risk of wall slip, especially for high consistency materials as mortars and soils [24,37,38]. The rotational strain amplitude was defined as 0.05%, at the linear viscoelastic region in strain sweep tests. The equipment was an Anton Paar MCR301 rheometer. The mortars were prepared according to the mixing procedure described by European standard EN-196-1. After mixing, the mortar was put in the rheometer cup, the excess material was removed with the use of a spatula and the cup was put in the machine for the test. The environmental conditions of the room were kept at 23±1°C and 50% RU; the rheometer temperature was kept at 23 ± 1°C. All tests were repeated 2 or 3 times.

2.3.3 Interfacial rheology

2.3.3.1 Definition and measurements

The interfacial measurements are based on Gibbs definition of surface, the "excess property" [39]. Assuming a monolayer at the surface of a liquid of elastic modulus of G_{bulk} and submitted to an oscillatory strain deformation. If we chose z as the vertical direction, shear deformation u along Ox direction varying along y, the strain rate γ is ∂u/∂y and the bulk shear stress is σ = G∂u/∂y in the small strain limit (linear regime). Close to the surface the local elastic modulus varies, and the stress can be described using an elastic modulus G(z) equal to G_{bulk} far from the surface and increasing close to the surface due to the presence of the monolayer [40]. The elastic modulus can be obtained by the equation:

$$G_{interface} = \int_{-\infty}^{0} [G(z) - G_{bulk}]dz - \int_{0}^{+\infty} [G(z)]dz \qquad (2)$$

where the position of the surface is the plane z = 0. This position is arbitrary, and is usually chosen so that the excess surface concentration of the liquid is zero [40].
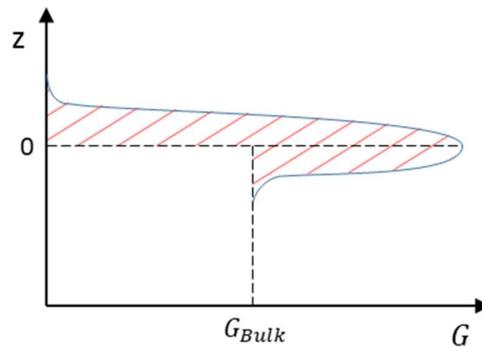

Figure 3. Schematic variation of elastic modulus near the surface; the area between the curve and the lines G(z < 0) = G_{bulk} and G(z > 0) = 0 is the surface elastic modulus $G_{interface}$.

Using these definitions, the evolution of interfacial viscoelastic properties was obtained through two measurements: one in which the vane geometry is partially immersed (3mm) including the interface and another with the geometry fully immersed in the bulk. The excess property is obtained by the difference between the measurement at 3mm and at the bulk. The bulk properties subtraction allows a closer

approach to the real interfacial properties. In this investigation, low amplitude storage modulus (G') and loss modulus (G'') were evaluated; they are defined as:

$$G'_{interface} = G'_{3mm} - G'_{bulk} \qquad (3)$$
$$G''_{interface} = G''_{3mm} - G''_{bulk} \qquad (4)$$

The bulk and interfacial configurations are shown in Figure 4. The 3 mm depth was chosen to be smallest as possible to minimize bulk effects, but large enough compared to grain size, about 6 times. The thicker the measurement, including the interface, the higher the bulk effects, and thus the measurement is less precise. The bulk effects are generally expressed by the boussinesq number [41]:

$$B_0 = \eta_s/\eta_{subph}L, \qquad (5)$$

where η_s is the surface viscosity, η_{subph} is the subphase viscosity and L the length scale associated with the measuring probe. When $B_0 \gg 1$, the drag experienced by the measuring probe dominates. When $B_0 \ll 1$, the properties of the surrounding phase dominate the drag force on the measuring probe, bulk phase contributions to the interfacial viscosity are relevant [41]. To minimize the bulk effect, the length scale is as small as possible, but kept at a minimal scale to obtain reliable data considering the grain size distribution.

Each formulation was then tested for 2h with a vane geometry at bulk (G'_{bulk}) and at the interface (G'_{3mm}) to calculate $G'_{interface}$. The test preparations and measurement conditions were the same as for bulk rheological measurements. The vane geometry advantage for this measurement was the possibility of using different depths, differently from other geometries as parallel plate, cone-plate, and bicone, where evaluating different depths or allowing evaporation to occur are not possible in a time sweep.
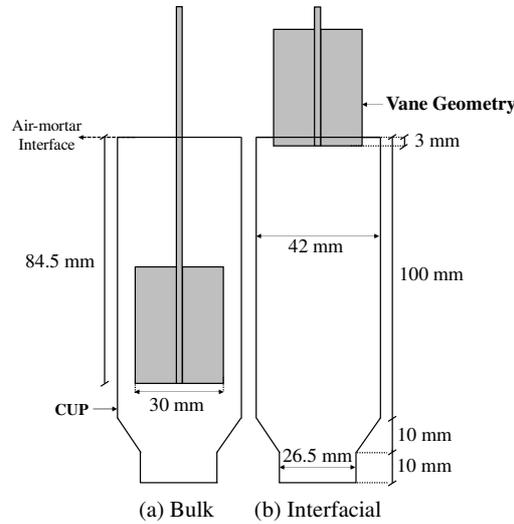

Figure 4. Scheme of the rheological measurements of adhesive mortars using a vane geometry: (a) bulk measurements were done at 84.5 mm depth; (b) interfacial measurements were done on the exposed mortar interface at 3 mm depth.

To perform the interfacial measurements with variations on the environmental conditions, an electric fan was introduced to produce wind and increase drying rate, as illustrated in Figure 5. The fan was positioned 2 meters away from the rheometer at velocity level 1.
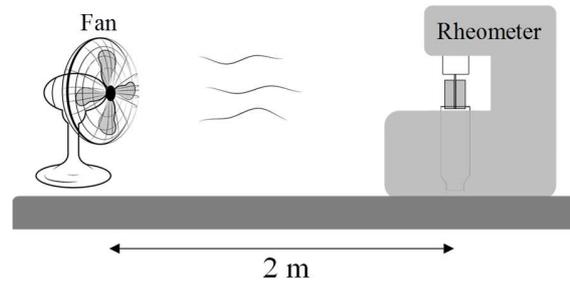
Figure 5. Scheme of interfacial rheology test in windy environmental condition.

2.3.4 Water evaporation

Water evaporation was assessed in mortar samples (cylinder of 6 mm height and 100 mm diameter) with the top uncovered. The mass loss was measured for 2 hours by an OHAUS precision scale with 0.01 g readability and registered by a data logger every 10 seconds. The test simulated the water loss at the interface, by limiting the volume to two times the thickness of the considered 3mm-top layer.

3 Results and discussion

3.1 MRI

3.1.1 2D MRI characterization of moisture spatial distribution

In Figure 6, the signal mitigation of moisture content inside a w_0.25% CE-A sample can be observed. Each image represents the signal intensity difference between the initial time (0 minute) and a specific moment (30 minutes, 1 hour and 2 hours). On the image, white areas represent zones where there is no difference in comparison to the reference and dark areas represent the zones where the signal had mitigation in relation to the reference, where free water is disappearing from water evaporating. MRI could evaluate the spatial distribution of moisture inside the sample through the depth and horizontal direction. With this result, it is possible to observe that during the first 2h the moisture vanishing grew from the surface to the inner layers of the material until 3 mm.
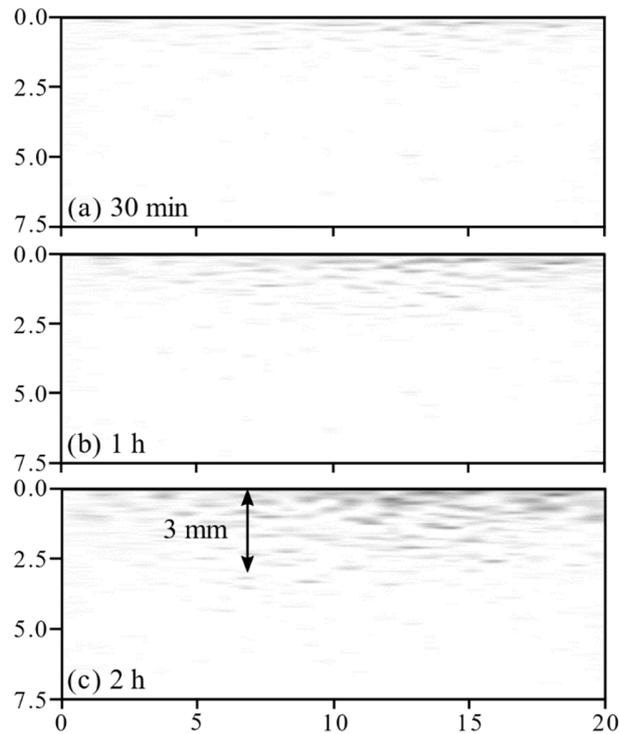
Figure 6. 2D MRI Result - 1ˢᵗ echo signal mitigation of water signal of an adhesive mortar sample (w_0.25% CE-A) exposed to air on the top: (a) water vanishing after 30 minutes; (b) water vanishing after 1 hour; (c) water vanishing after 2 hours.

The relative humidity during MRI measurements was lower than the value during other types of tests (rheology and water evaporation), at 30% instead of 50% of RU, which could not be changed. This condition could have an influence on intensifying water evaporation during MRI; however, this result can offer an approximation of water distribution during skin formation.

The MRI technique provides detailed information of water distribution in a section cut, showing the water concentration diminishing along the vertical axis due to drying, but it does not take in account the entire sample as the measurements focus only on the central plane. For the skin formation matter, having quantitative information of the entire sample would provide more complete information.

3.1.2   MRI characterization of moisture distribution along the depth

In Figure 7a, 7b and 7c, the distribution of the free water's signal intensity over time is shown for the formulations with different CE content. In the images, each vertical line represents the distribution of signal intensity through the depth that was acquired every 5 minutes. While blue represents low signal intensities (dryer material), red represents higher signal intensities (moisturized material), as shown on the color scale.

Figure 7a shows the formulation with lower CE content, w_0.1% CE-A, where the moisture distribution through the depth is fairly homogeneous. In comparison to other samples, the signal intensity along the whole sample reduces considerably during the first 2h. This indicates that the mortar loses water from the surface by evaporation, but the moisture inside is able to move and re-homogenize.
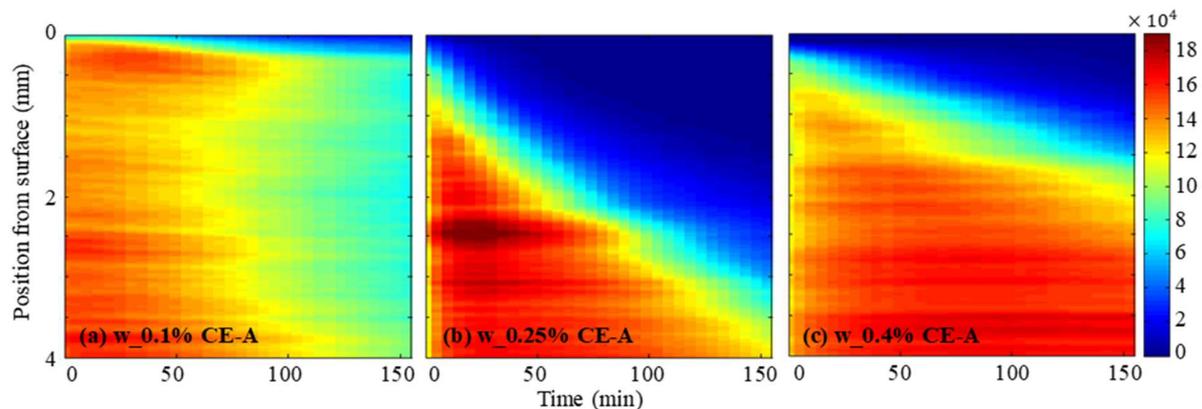
Figure 7. 1D MRI Result – 1ˢᵗ echo map signal vs time of adhesive mortar samples exposed to air on the top: (a) W_0.1% CE-A; (b) W_0.25% CE-A; (c) W_0.4% CE-A

The result of the w_0.25% CE-A formulation is shown in Figure 7b. A low signal layer linearly grows toward the inner part of the sample as a function of elapsed time and the dark blue area indicates a dry layer. The material that is located below this dryer zone has a more intense signal, showing that underneath the mortar keeps its moisture content. This result is different from w_0.1% CE-A, where the material does not form these two zones of dry and moisturized mortar, staying homogeneous from the top to the bottom of the sample with higher mitigation of the water signal measured on the bottom of the sample for longer times. The nature of CE explains these results, as it forms an aqueous phase with higher viscosity that reduces water mobility [27,42], consequently inhibiting water flow towards the mortars surface. This means that as the mortar with higher CE content started to lose water from the surface, a layer of dryer material formed; this drying layer grew down the surface, but the material below this layer retained its moisture.

For w_0.1% CE-A, on the other hand, as water evaporates, free water freely migrates in the direction of the surface, remoisturizing the top layers, obtaining a dryer, but homogeneous sample. At 2h, similarly to the 2D MRI in section 3.1.1, the w_0.25% CE-A layer had approximately 3 mm of dryness; thus, the results obtained from both methods (2D and 1D MRI) were consistent.

The w_0.4% CE-A formulation, with even higher CE content, also presented the linear formation of the dry layer material evolving with time toward the inner layers of the sample, similarly to w_0.25% CE-A. However, the growing rate was less than the other sample and after 2h the dry layer was only 1.5 mm thick, which is smaller than the 3 mm seen for w_0.25% CE-A. The slower growing rate and final thickness of the dry zone may be related to the higher CE content (0.4%), which intensifies polymer film formation that creates a barrier to water evaporation. This result reinforces CE's water retention ability, and by its increase, less water is lost from the mortars.

Bülichen et al. [2] studied methyl hydroxyethyl cellulose (MHEC) water retaining ability and identified two effects: the water sorption and the formation of a hydrocolloidal associated 3D polymer network, which may be the barrier that is reducing the rate of skin formation. Results from Jenni et al. [4], Bühler et al. [5] and Faiyas et al. [32] also indicated the formation of a polymer film at the granular structure. Jenni et al. [4] observed polymer enrichment at mortar's surface due to water flow towards the surface with evaporation and skin formation, while Zurbriggen et al. [6] concluded that the flow of water towards the evaporation front did not only transport organics, but also cementitious ions which did enrich the evaporation front and locally caused early precipitation of hydrates and carbonates. The present results confirms that the skin is present from the beginning as observed by Bühler et al. [5] and that the buildup

of the crust is in the order of 0.5-1 mm within the first 30 min as observed Zurbriggen et al. [6]. In the present work, while the redispersible polymer powder is constant, the CE concentration is different for each formulation, and higher concentration could lead to earlier formation of polymer film barrier that prevents water evaporation. Thus, the present results cannot confirm or deny the hypothesis of organic transportation.

For adhesive mortars, the higher the CE content, the higher the skin rigidity. However, MRI results indicate that for 0.4% of CE, the dry layer formed is thinner than that of the composition with 0.25%; thus, the rheological properties of the skin are not only related to its thickness. Early precipitation, polymer enrichment, film formation and carbonation at the interface could influence rheological properties of the dry layer.

3.2 Bulk rheology

In this section, results of bulk rheological properties are shown and analyzed. The impact of different CE content on bulk rheological properties of mortar with gray and white cement is discussed. Then, the results of mortars with different degree of substitution's CE are shown and discussed.

3.2.1 Effect of CE content

In Figure 8, G' and G'' evolution over time for white cement (a) and gray cement (b) mortars with different CE-A content are shown. In the graph, equal color and shape curves represent a repetition. The Loss modulus values have an inversed tendency compared to storage modulus, since w_0.4% CE-A has higher values than w_0.25% CE-A and w_0.1% CE-A. These results' order of magnitude is much lower than the storage modulus since the elastic behavior is dominant. Thus, in the next sections, the G' will be mainly explored.

In the first minutes, for both types of cement, G' of the different CE content formulations are similar, with 0.25% CE-A being the lowest, then 0.4% CE-A in the middle, and 0.1% CE-A the highest. The reduction of the initial G' values of 0.1% and 0.25% CE-A is related to the air entraining effect of CE. From 0.1% to 0.25% CE-A, entrained air increases from 14% to 19% for white cement and 13% to 20% for gray cement (Table 4). For 0.4% CE-A, however, air entrainment seems to have almost saturated, and the entrained air obtained is 21% for white cement and 22% for gray cement. The air entrainment effect is diminished at higher concentrations, the polymer thickening effect starts to influence, and G' becomes higher for higher CE-A content.

After around 8-10 minutes, an inversion of G' values occur. The formulation with higher CE content, 0.4% CE-A, became lower than 0.25% CE-A, and maintained lower values during the 2 hours of the test. This low value is probably related to the CE's ability to delay structuring of cement particles [28]. Weyer et al. [21] showed that the adsorption of the polymers onto the cement clinker phases inhibits the formation of $Ca(OH)_2$. This is related to CE's strong influence on C-S-H precipitation, leading to a decrease in the amount of initial C-S-H nuclei, delaying the formation of a continuous C-S-H shell around the C_3S grain, and delaying the formation of a thicker and more permeable C-S-H layer.

When CE is added to a cementitious matrix, a gradual reduction of C_3A dissolution rate is observed; this is also associated with AFt and hydroxy-AFm precipitation [21,28]. Often the increase of viscosity generated by CE is associated with hydration retardation, however, Pourchez et al. [114] results have shown that the assumption of a diffusion barrier induced by the high viscous solution of cellulose ethers is not relevant.
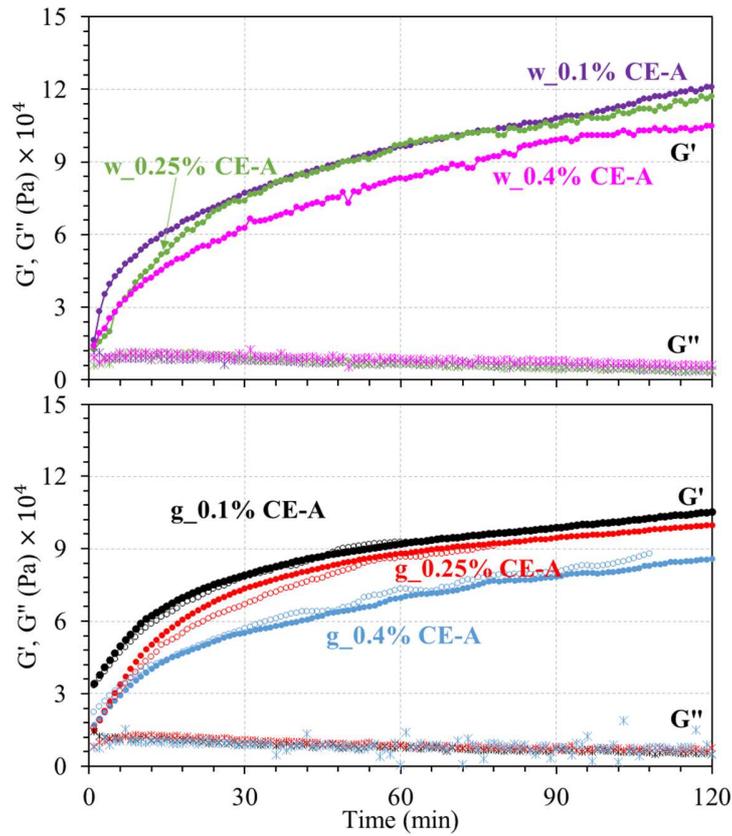
Figure 8. Storage modulus (G') and Loss modulus (G") of adhesive mortars with different CE content formulated with white cement (a) and gray cement (b).

To ensure the effect of the polymer concentration observed in the initial minutes, a series of tests with a wider range of dosages (0.1%, 0.2%, 0.25%, 0.3%, 0.4%, 0.5%) of CE were performed for gray cement and shown in Figure 9. From the initial start (t = 1 minute), from 0.1% to 0.25%, the G' values decrease as dosage increases; it is related to the increase of air content, due to CE's air entraining ability. From 0.25% to 0.5%, however, the air content achieves saturation and remains stable; and as dosage increases, G' values increase, which is explained by CE's thickening effect. These results confirm the behavior observed earlier in Figure 8 with white and gray cement.
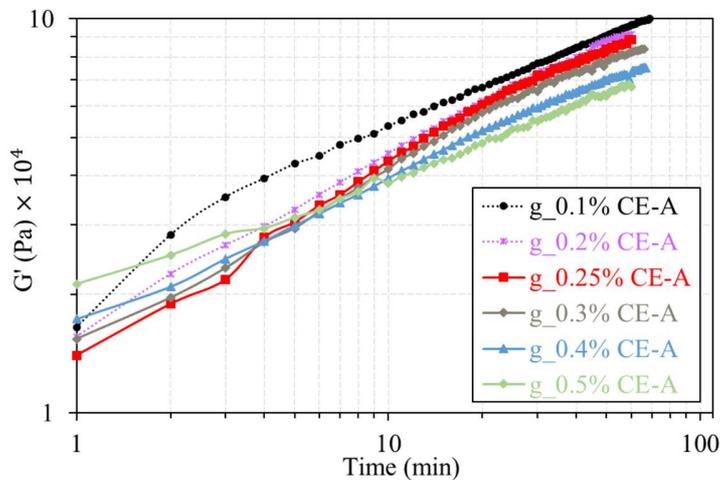
3.2.2 Effect of CE types

CE is already known to delay cement hydration [13,27], and the degree of substitution (DS) is related to this effect [1]. In this section, the influence of CE type on bulk oscillatory properties of adhesive mortar with white and gray cement is evaluated.

In both types of cement, similar results can be observed in Figure 10 regarding the influence of DS on G' evolution. For both cements, the initial point of the three curves starts at the same place. This is expected since the three polymers have similar nominal viscosity and similar air entrained values. The first points represent the material just after mixing, and similar behavior is observed regardless of the DS. After the initial point, the formulation with CE-B delayed G' evolution for both cements. CE-C in both cases had a low impact on G' evolution, and in both cement types, higher G' values are observed. CE-A, however, had a slightly different effect depending on cement type. CE-A seems to have an intermediate impact in comparison to the other CE types, but for white cement, it was closer to CE-C and for gray cement, it was closer to CE-B.

The obtained results regarding the DS outcome indicate that polymer with higher DS has a stronger delay on G' evolution. As shown in Table 3, CE-B has the highest DS, around 1.8-1.9, followed by 1.62-1.65 for CE-A and 1.4 for CE-C. This result, however, is not compatible with what is found in literature. Weyer et al. [43] concluded that the lower the DS of the polymer, the stronger the retardation of C_2S/C_3S-hydration. The latter disagrees with results obtained in this investigation, where lower DS resulted in lower retardation of structuring.

The disagreement between literature and this investigation can be related to other characteristics that were not provided by the manufacturers such as molecular weight, degree of polymerization, and positioning of the free hydroxyl groups. Manufacturers of commercially available CEs generally do not provide some of the information for confidentiality reasons [1]. Thus, even though the degrees of polymerization of the CEs in this research were not provided, it may have an influence on rheological property evolution. Pourchez et al. [44] verified that hydroxyethyl cellulose (HEC) with different molecular weights and similar degrees of substitution have negligible effects on cement hydration. The same parameter's impacts are also applied to hydroxyethyl methyl cellulose (HEMC), so perhaps molecular weight may not be the dominant parameter. The positioning of the free hydroxyl groups in cellulose ether molecules could influence the structuring process; however, other factors could also have an influence. Thus, verification is necessary.
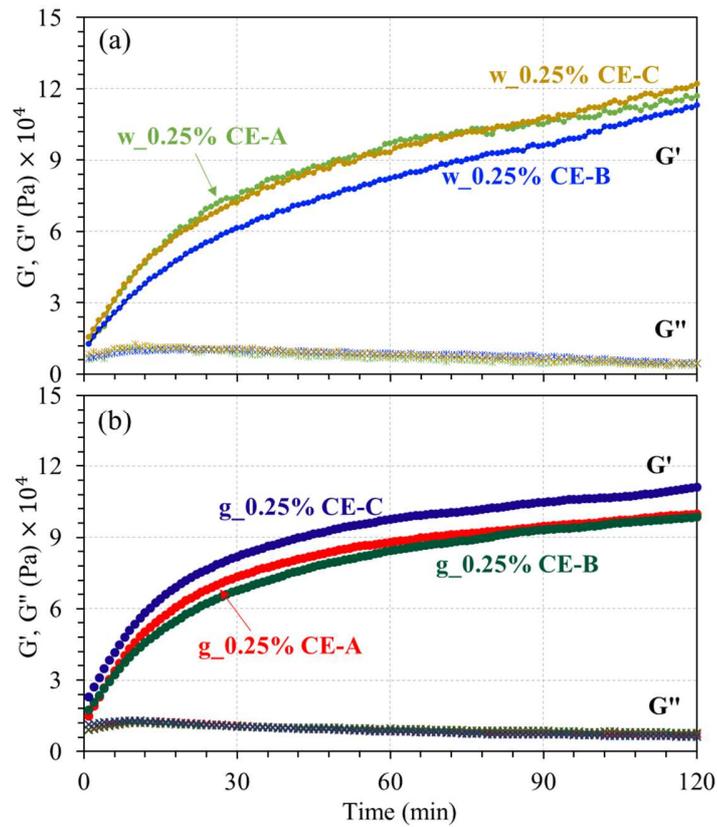
Figure 10. Storage modulus (G') and Loss modulus (G") of adhesive mortars with different CE types formulated with white cement (a) and gray cement (b).

As shown in Figure 10, the CE-A had a different impact on G' structuring depending on the cement type. This is probably related to the differences of the phases of each cement. From Table 2, while both cements have similar C_3S content (white cement – 58%; gray cement – 61%), C_2S is about 2 times higher for white cement (white cement – 28%; gray cement – 14.3%). Since CE affects C_3S and C_2S hydration, it is expected that the polymers have a different effect on hydration and, consequently, influence the structure building of the mortar. Previous research demonstrated that CE adsorption is phase-specific and HEMC polymers also have impacts on the C_3A phase, even though HEMC's influence is lower than HEC polymers [45]. Since gray cement C_3A content is 2 times higher than white cement (white cement – 6%; gray cement – 12%), this is probably another source of variation on the effect.

The impact of the DS is not fully understood, and further studies would be necessary to explain the behavior showed in this investigation. Molecular length measurements would be a possible approach to further understand the results.

3.3 Interfacial rheology of skin

In this section, the results of the introduced technique, interfacial rheology for adhesive mortars, are discussed. Three parameters are evaluated that influence the interfacial properties of mortars with white cement and gray: CE content, DS of CE, and environmental conditions.

3.3.1 Effect of CE content

In Figure 11a, the obtained results are shown with the vane fully immersed, at the bulk (G'_{bulk}), and the vane partially immersed at 3 mm (G'_{3mm}) of the interface for formulations with white cement and different

CE content. It is clear from the graph that the measurements difference is about one order of magnitude, indicating that the properties of the interface increase faster. The number of boussinesq in this case is, $B_o \cong 10 \gg 1$; the properties of the interface are dominant in the measurements. From equation 2, $G'_{interface}$ was obtained from the difference of G'_{3mm} and G'_{bulk} and shown in Figure 11b. Water loss was also plotted in Figure 11b.
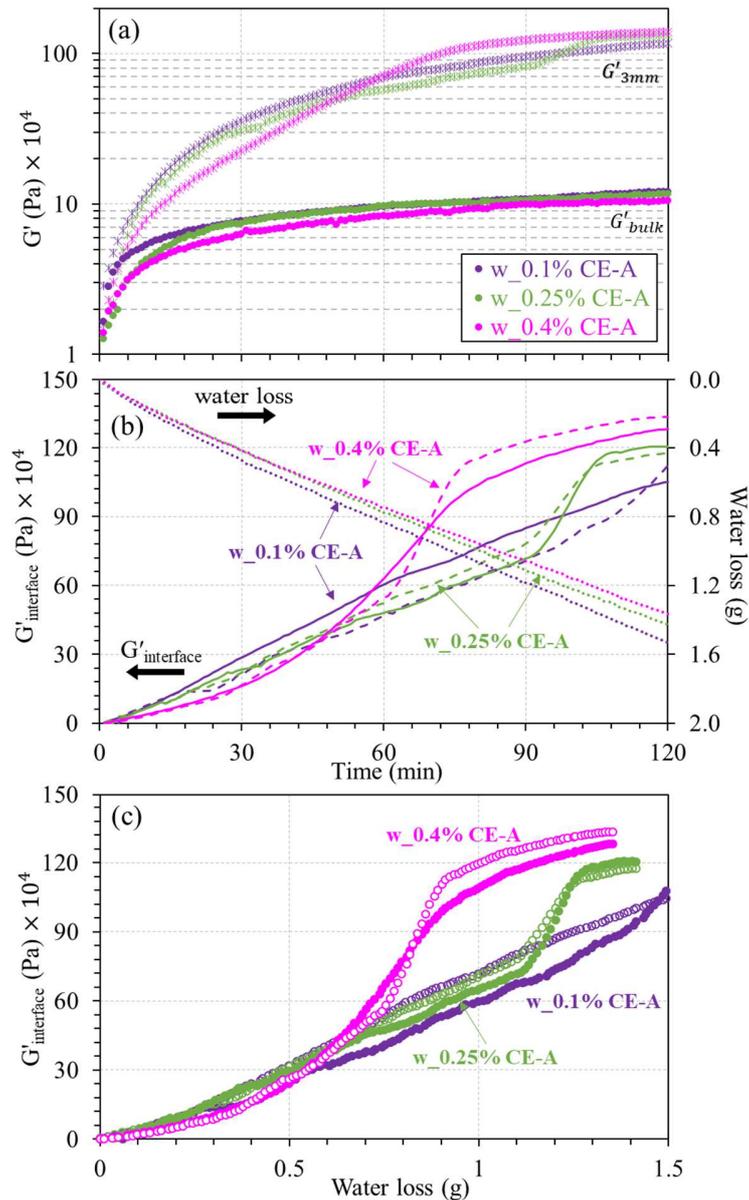

Figure 11. (a) Bulk measurements (G'_{bulk}) and 3mm measurements (G'_{3mm}) of adhesive mortars with different CE content formulated with white cement; (b) $G'_{interface}$ calculated by the different of the G'_{3mm} and G'_{bulk}; and (c) $G'_{interface}$ vs water loss from (b) (curves with same color in (b) and (c) represent a repetition).

In the first 30 minutes, the $G'_{interface}$ of all formulations has a linear increase, and the higher the CE content, the smaller the rate. The formulation with lower CE, w_0.1% CE-A remains linear during the entire test. Around 90 minutes, w_0.25% CE-A has an inflection and its values also increase at a higher

rate, but stay between w_0.1% CE-A and w_0.4% CE-A. Between 30 and 60 minutes, the w_0.4% CE-A curve has an inflection and its values achieve higher values than the other formulations.

Similar results regarding the influence of CE on the interfacial properties on $G'_{interface}$ can be observed for gray cement in Figure 12a. g_0.1% CE-A presented a linear increase during the entire test. In the other formulations, g_0.25% CE-A and g_0.4% CE-A, a period of linear evolution occurs in the beginning. In this first linear period, the higher CE content, the lower $G'_{interface}$ increase slope. After a linear period, the formulations with higher CE content, g_0.25% CE-A and g_0.4% CE-A, show an inflection and change their increase rate. For g_0.25% CE-A, the inflection occurs around 75 minutes, while for g_0.4%CE-A, around 60 minutes. At the end of the test, at 2h, the formulation with higher CE content, g_0.4% CE-A, achieves the highest values, followed by g_0.25% CE-A and g_0.1% CE-A.

Results indicate that higher CE content in the formulation initially generates a reduction on rheological property evolution of the interface, but it induces a higher final value. This is explained by CE's water retaining effect, which delays water/solids concentration decrease of the mortars with higher concentration of CE, and consequently delaying $G'_{interface}$ evolution. In Figure 12b, the same $G'_{interface}$ results correlated with the water loss for each cement type formulation are shown. This correlation reinforces that during a first moment, the interface evolution is related to water loss and increases linearly, but for the formulations with higher CE content, an inflection occurs. This inflection is related to a polymer property's dominance. The higher the concentration, the earlier this inflection occurs; therefore, the effect is seemingly related to the polymer concentration.
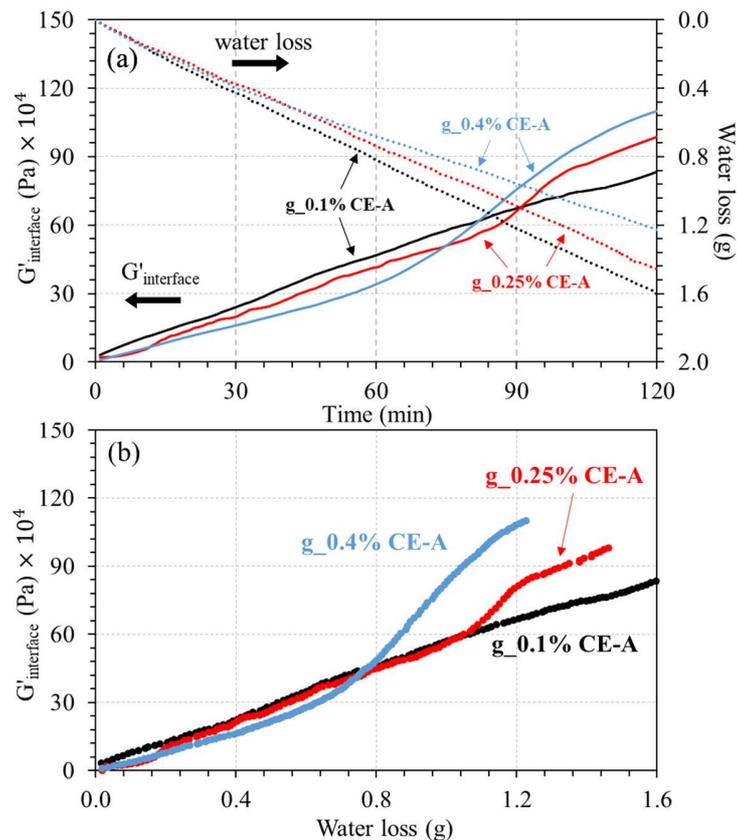

Figure 12. (a) $G'_{interface}$ of adhesive mortars with different CE content formulated with gray cement and curves of water loss over time of each formulation (b) $G'_{interface}$ vs water loss of adhesive mortars with different CE content formulated with gray cement.

MRI results in Figure 7 reinforce that the change in behavior is related to the polymer dominance. One can observe that compared to w_0.25% CE-A, w_0.4% CE-A has smaller dryer layers; however, the interfacial properties show that during this period, the higher CE content got a much higher storage modulus (G'). This indicates that in the first 30 minutes, the interfacial properties are related to water/solids concentration and evaporation, but then the polymer film, other early hydrates or carbonation start to influence rheological properties.

The results of $G'_{interface}$ divided by water loss at the end of the test for both series with gray and white cement are shown in Figure 13 as a function of CE content. The increasing tendency of the $G'_{interface}$/water loss shows that $G'_{interface}$ increase is not only related to water loss, but also to the effect of CE content on the skin composition.

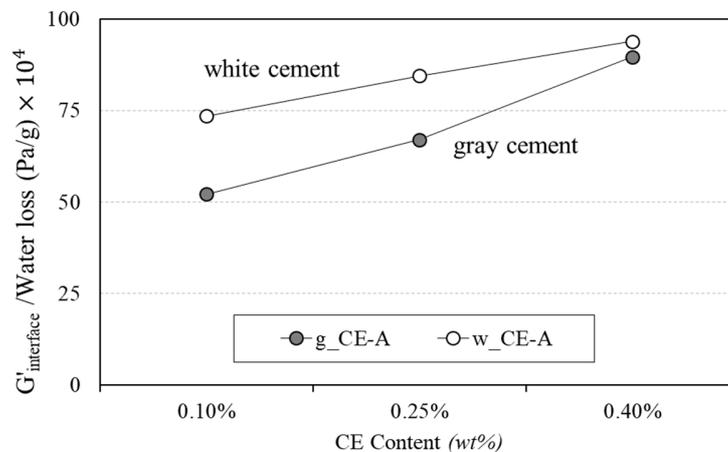*Figure 13. $G'_{interface}$/Water loss vs CE content at t = 2 hours of formulations with grey and white cement.*

Finally, the introduced method was able to extract a clear difference between the various formulations and enabled quantification of the rheological properties of the skin. Thus, it was possible to verify the level of influence that CE content has on skin properties.

3.3.2 Effect of CE type

In Figure 14a, $G'_{interface}$ of white cement formulations with different CE types and water loss over time are shown. The water loss is represented with dotted lines; from the curves, it appears that the type of CE did not have a considerable effect on water evaporation. Their nominal viscosities are equal, but have a different DS and MS. It did not affect the water loss considerably; however, the interfacial property's evolution presents some small differences.

In Figure 14b, $G'_{interface}$ of gray cement formulations with different CE types and water loss over time are shown. Compared to white cement, the water loss results do not show a considerable change between the different CEs. For the gray cement, however, the differences on skin rheological properties are clearly noted. For g_0.25% CE-B, an inflection occurred around 60 minutes, earlier than g_0.25% CE-A and g_0.25% CE-C at 90 minutes. This result may reinforce that the polymer properties start to be dominant and then an inflection occurs. These results indicate that the type of CE can have a different influence on skin formation depending on the cement type. The technique could also enable studies for comparing different polymers and predict non-performant raw materials.
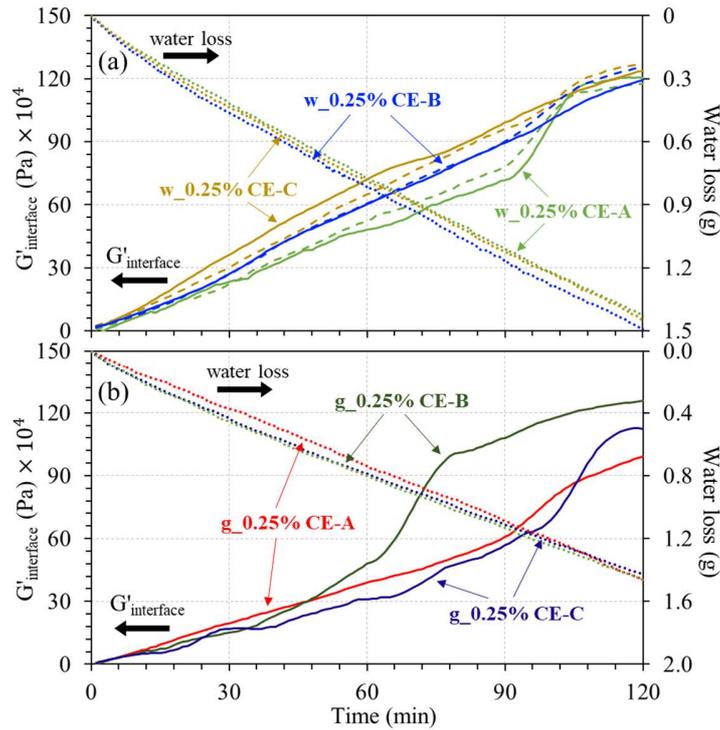
Figure 14. G'_{interface} of adhesive mortars with different CE types formulated with white cement (a) and gray cement (b). Each color represents a type; continuous and dashed lines are test repetitions. Water loss over time of the same formulations is represented by dotted curves.

3.3.3   Wind effect for gray cement

In Figure 15, $G'_{interface}$ of white cement formulations with different CE contents subjected to two different environmental conditions, with and without wind, are shown. The samples in windy conditions are represented with continuous lines and normal conditions with dashed lines. The graph shows that at windy conditions, g_0.1% CE-A has a linear increase until 45 minutes when it starts to get into a plateau; in non-windy conditions, it linearly increases during the whole experiment.

In the case of g_0.25% CE-A in windy conditions, for 20 minutes there is a linear increase and then inflection occurs with a high increase of G' until 60 minutes when it gets into a plateau. During non-windy conditions, this occurs at 90 minutes and has a faster increasing rate until the end of the test.

In windy conditions, g_0.4% CE-A has a similar behavior to g_0.25% CE-A. The formulation with 0.4% CE has a smaller increase rate in the first 20 minutes, but after the inflection, it has a strong acceleration and at 40 minutes overcomes g_0.25% CE-A (Wind) then starts a plateau. In non-windy conditions, the smaller rate in the beginning also happens until the inflection point where it accelerates and overcomes the other CE content formulations.
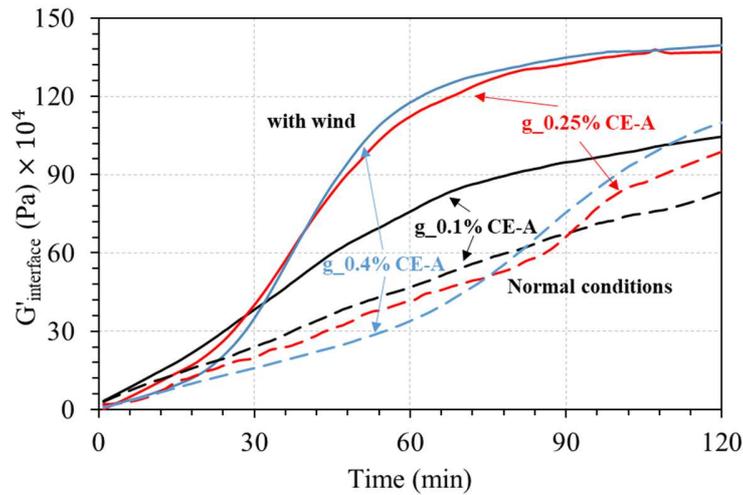
Figure 15. Interfacial storage modulus of adhesive mortars with different CE content in windy conditions (continuous line) and the reference without wind (dashed lines)

It seems that when comparing wind and non-wind conditions, all formulations have a similar behavior with a linear evolution rate until they have an inversion of behavior where the highest CE properties overcome the others. However, in windy conditions, this process took place earlier, since wind accelerates water evaporation.

This result can be compared to an application condition where evaporation is intensified, not only in a windy condition, but in other environments such as exterior tiling (swimming pool, terrace, façade, etc), with lower humidity and higher temperature. Under these conditions, evaporation process increases and therefore the evolution of interfacial properties is also increased.

4   Conclusion

An investigation regarding the formation of skin layer on fresh adhesive mortar has been undertaken. The association of MRI, evaporation measurements and rheology techniques allowed the evaluation of the influence of cellulose ether (CE) content, different CE types, and environmental conditions on the formation dynamics of the skin and the evolution of its rheological behavior. MRI was employed to assess the water distribution within the mortar specimens including the air-mortar interface. It was possible to observe that for low content, as low as 0.1% CE, despite the higher evaporation rate, a dryer layer did not form until 1 hour, and after 2 hours it was very thin or related to retraction, around 0.2 mm. For higher CE contents however, a dryer layer formed linearly, around 3 mm for w_0.25% CE-A and 1.5 mm for w_0.4% CE-A after 2 hours. The MRI results also shown that for 0.1% CE the distribution of water content was more homogenous though the depth, thus a drying layer was not formed at the surface. This shows that probably the 0.1% content allowed water in the sample to be mobile and rehomogenize.

The rheological evaluation of bulk properties indicated that in the very beginning air entrainment predominantly influenced the mortar when smaller dosages of CE were used, from 0.1% to 0.25%. For 0.40% of CE, the air entrainment saturation was reached and the polymer effects increased G' initial value. However, CE also delays the structuring process of cement particles, which generates an inversion for the content above 0.25%. Finally, after about 3 minutes the tendency is that the higher the CE content, the lower G'.

Regarding the cellulose ethers with different DS, the delay of G' evolution was stronger for mortars with CE of higher DS. Further investigation is necessary since this measured effect contradicts the published literature.

An interfacial rheology technique for mortars was introduced in this work, aiming to evaluate the skin rheological behavior during the first two hours. The technique was able to quantitatively compare different formulations and conditions. For different CE contents, it was observed a transition from a water/solids concentration dominance to a polymer properties dominance on the rheological properties of the skin in mortars with two different cements. Higher CE contents induce less water evaporation, thus higher water/solids ratios, which dominates the skin behavior in a first moment, resulting in smaller G' values. Then, in a second moment, the polymer properties start to dominate, and higher contents induce higher G' values. The results lead to the conclusion that even though the water evaporation differences and their direct influence on interfacial properties due to water/solids reduction are relatively small, their impact on rheological properties of the interface in a system with high CE concentration are potentialized by the formation of dry skin where the polymer properties start to dominate.

When CE with different degrees of substitution were evaluated, different inflection times were observed despite the similar viscosity of the polymers and water evaporation rate. Under different environmental conditions, similar behaviors of the mortars were verified, but with accelerated evolution when windy conditions were applied.

This new interfacial rheological method for suspensions can be useful to evaluate the influence of different conditions and mix designs, to better understand skin formation, and to improve adhesive mortar's performance. For instance, further research should be conducted to verify the interaction of redispersible polymer powder and CE on interfacial properties. Moreover, interfacial rheology also presents interesting potential to be employed to other granular systems, in which surface evolution is relevant. This is the case for rendering mortars, external wall insulation system (EWIS), concrete, concrete repair layers, 3D printing, etc.

5 Acknowledgements

6 References

[1]   J.-Y. Petit, E. Wirquin, Evaluation of various cellulose ethers performance in ceramic tile adhesive mortars, Int. J. Adhes. Adhes. 40 (2013) 202–209. doi:10.1016/j.ijadhadh.2012.09.007.

[2]   D. Bülichen, J. Kainz, J. Plank, Working mechanism of methyl hydroxyethyl cellulose (MHEC) as water retention agent, Cem. Concr. Res. 42 (2012) 953–959. doi:10.1016/j.cemconres.2012.03.016.

[3]   M. Cappellari, A. Daubresse, M. Chaouche, Influence of organic thickening admixtures on the rheological properties of mortars: Relationship with water-retention, Constr. Build. Mater. 38 (2013) 950–961. doi:10.1016/j.conbuildmat.2012.09.055.

[4]   A. Jenni, L. Holzer, R. Zurbriggen, M. Herwegh, Influence of polymers on microstructure and adhesive strength of cementitious tile adhesive mortars, Cem. Concr. Res. 35 (2005) 35–50. doi:10.1016/j.cemconres.2004.06.039.

[5]   T. Bühler, R. Zurbriggen, U. Pieles, L. Huwiler, R.A. Raso, Dynamics of early skin formation of

tiling mortars investigated by microscopy and diffuse reflectance infrared Fourier transformed spectroscopy, Cem. Concr. Compos. 37 (2013) 161–170. doi:10.1016/j.cemconcomp.2012.10.008.

[6]   R. Zurbriggen, T. Bühler, U. Pieles, A. Wetzel, M. Herwegh, Dynamics of Skin Formation and Mechanisms of Open Time Performance of Tile Adhesive Mortars, in: F. Leopolder (Ed.), Drymix Mortar Yearb. 2013 - Proc. Idmmc Four, Nuremberg, Germany, 2013: pp. 76–79.

[7]   CEN, EN 1347: Adhesives for tiles — Determination of wetting Capability, Eur. Stand. (2007).

[8]   R. Zurbriggen, M. Herwegh, U. Pieles, T. Bühler, L. Huwiler, A new laboratory method to investigate skin formation and Open Time performance, in: Third Int. Drymix Mortar Conf. Idmmc Three, Nürnberg, Germany, 2011: pp. 1–8.

[9]   Y.V. Póvoas, Avaliação da Formação de "Película" na Argamassa Colante e sua Influência na Adesão, University of São Paulo, 2005.

[10]   M.R.M.M. Costa, E. Pereira, R.G. Pileggi, M.A. Cincotto, Study of the influential factors on the rheological behavior of adhesive mortar available in the market, Ibracon Struct. Mater. J. 6 (2013) 399–405.

[11]   T. Poinot, M.C. Bartholin, A. Govin, P. Grosseau, Influence of the polysaccharide addition method on the properties of fresh mortars, Cem. Concr. Res. 70 (2015) 50–59. doi:10.1016/j.cemconres.2015.01.004.

[12]   H. Paiva, L.M. Silva, J.A. Labrincha, V.M. Ferreira, Effects of a water-retaining agent on the rheological behaviour of a single-coat render mortar, Cem. Concr. Res. 36 (2006) 1257–1262. doi:10.1016/j.cemconres.2006.02.018.

[13]   A.M. Betioli, P.J.P. Gleize, D.A. Silva, V.M. John, R.G. Pileggi, Effect of HMEC on the consolidation of cement pastes: Isothermal calorimetry versus oscillatory rheometry, Cem. Concr. Res. 39 (2009) 440–445. doi:10.1016/j.cemconres.2009.02.002.

[14]   J.Y. Petit, B. Comelli, R. Perrin, E. Wirquin, Effect of formulation parameters on adhesive properties of ANSI 118-15 and 118-11 compliant tile adhesive mortars, Int. J. Adhes. Adhes. 66 (2016) 73–80. doi:10.1016/j.ijadhadh.2015.12.011.

[15]   P. Whittingstall, Measuring The Viscosity Of Non-Newtonian Fluids, Handb. Food Anal. Chem. 2–2 (2005) 375–383. doi:10.1002/0471709085.ch25.

[16]   R. Zurbriggen, L. Huwiler, T. Bühler, U. Pieles, A. Wetzel, M. Herwegh, Early mechanisms at mortar surfaces: Skin formation and adhesion properties, in: D. Stephan, H. von Daake, V. Märkl, G. Land (Eds.), Monographien, Berlin, Germany, 2013: p. vol. 46, pgs 145-148.

[17]   J W Costerton, K J Cheng, G G Geesey, T I Ladd, J C Nickel, M Dasgupta, et al., Bacterial Biofilms in Nature and Disease, Annu. Rev. Microbiol. 41 (1987) 435–464. doi:10.1146/annurev.mi.41.100187.002251.

[18]   J. Krägel, S.R. Derkatch, Interfacial shear rheology, Curr. Opin. Colloid Interface Sci. 15 (2010) 246–255. doi:10.1016/j.cocis.2010.02.001.

[19]   J. Krägel, S.R. Derkatch, R. Miller, Interfacial shear rheology of protein-surfactant layers, Adv. Colloid Interface Sci. 144 (2008) 38–53. doi:10.1016/j.cis.2008.08.010.

[20]   R. Miller, L. Liggieri, Interfacial Rheology, (2009) 1–24.

[21]   Y. Fan, S. Simon, J. Sjöblom, Interfacial shear rheology of asphaltenes at oil-water interface and its relation to emulsion stability: Influence of concentration, solvent aromaticity and nonionic

surfactant, Colloids Surfaces A Physicochem. Eng. Asp. 366 (2010) 120–128. doi:10.1016/j.colsurfa.2010.05.034.

[22]   S. Reynaert, C.F. Brooks, P. Moldenaers, J. Vermant, G.G. Fuller, Analysis of the magnetic rod interfacial stress rheometer, J. Rheol. (N. Y. N. Y). 52 (2008) 261. doi:10.1122/1.2798238.

[23]   G.G. Fuller, Rheology of Mobile Interfaces, Rheol. Rev. 2003 (2003) 77–123.

[24]   A. Kaci, R. Bouras, M. Chaouche, P.A. ani, H. Brossas, Adhesive and rheological properties of mortar joints, Appl. Rheol. 19 (2009) 51970.

[25]   M. Wyrzykowski, R. Kiesewetter, J. Kaufmann, R. Baumann, P. Lura, Pore structure of mortars with cellulose ether additions - Mercury intrusion porosimetry study, Cem. Concr. Compos. 53 (2014) 25–34. doi:10.1016/j.cemconcomp.2014.06.005.

[26]   A. Izaguirre, J. Lanas, J.I. Álvarez, Characterization of aerial lime-based mortars modified by the addition of two different water-retaining agents, Cem. Concr. Compos. 33 (2011) 309–318. doi:10.1016/j.cemconcomp.2010.09.008.

[27]   K.H. Khayat, Viscosity-enhancing admixtures for cement-based materials — An overview, Cem. Concr. Compos. 20 (1998) 171–188. doi:10.1016/S0958-9465(98)80006-1.

[28]   A.M. Agrawal, R. V. Manek, W.M. Kolling, S.H. Neau, Water distribution studies within microcrystalline cellulose and chitosan using differential scanning calorimetry and dynamic vapor sorption analysis, J. Pharm. Sci. 93 (2004) 1766–1779. doi:10.1002/jps.20085.

[29]   C. Marlière, P. Faure, P. Coussot, D. Vlassopoulos, A. Larsen, B. Loppinet, Jamming of cellulose ether solutions in porous medium, AIChE J. 61 (2015) 3923–3935. doi:10.1002/aic.14920.

[30]   B. Rånby, R. Noe, Crystallization of cellulose and cellulose derivatives from dilute solution. I. Growth of single crystals, J. Polym. Sci. 51 (1961) Abadi, Mohammad Tahaye. 2009. "Micromechanical Ana. http://onlinelibrary.wiley.com/doi/10.1002/pol.1961.1205115520/full.

[31]   M. Fourmentin, P. Faure, S. Rodts, U. Peter, D. Lesueur, D. Daviller, et al., NMR observation of water transfer between a cement paste and a porous medium, Cem. Concr. Res. 95 (2017) 56–64. doi:10.1016/j.cemconres.2017.02.027.

[32]   A.P.A. Faiyas, S.J.F. Erich, H.P. Huinink, O.C.G. Adan, T.G. Nijland, Effect of MHEC on evaporation and hydration characteristics of glue mortar, Cem. Concr. Res. 83 (2016) 97–103. doi:10.1016/j.cemconres.2016.01.010.

[33]   S. Jarny, N. Roussel, S. Rodts, F. Bertrand, R. Le Roy, P. Coussot, Rheological behavior of cement pastes from MRI velocimetry, Cem. Concr. Res. 35 (2005) 1873–1881. doi:10.1016/j.cemconres.2005.03.009.

[34]   B.M. Dale, M.A. Brown, R.C. Semelka, MRI Basic Principles and Applications, John Wiley & Sons, Ltd, Chichester, UK, 2015. doi:10.1002/9781119013068.

[35]   B. Mackiewich, Intracranial Boundary Detection and Radio Frequency Correction in Magnetic Resonance Images, University of British Columbia, 1990.

[36]   H.A. Barnes, Q.D. Nguyen, Rotating vane rheometry — a review, J. Nonnewton. Fluid Mech. 98 (2001) 1–14. doi:10.1016/S0377-0257(01)00095-7.

[37]   Q.D. Nguyen, D. V. Boger, Thixotropic behaviour of concentrated bauxite residue suspensions, Rheol. Acta. 24 (1985) 427–437. doi:10.1007/BF01333970.

[38]   H.A. Barnes, A review of the slip (wall depletion) of polymer solutions, emulsions and particle suspensions in viscometers: its cause, character, and cure, J. Nonnewton. Fluid Mech. 56 (1995) 221–251. doi:10.1016/0377-0257(94)01282-M.

[39]   J.W. Gibb, The collected works, Longmans, Green & Co., 1928.

[40]   D. Langevin, Surface shear rheology of monolayers at the surface of water, Adv. Colloid Interface Sci. 207 (2014) 121–130. doi:10.1016/j.cis.2013.10.030.

[41]   J. Mewis, N.J. Wagner, Colloidal Suspension Rheology, Cambridge University Press, 2012. doi:10.1017/CBO9780511977978.

[42]   L. Patural, A. Govin, P. Grosseau, B. Ruot, O. Devès, The effect of cellulose ethers on water retention in freshly-mixed mortars, in: 11th Int. Conf. Exhib. Eur. Ceram. Soc. 2009, 2009: pp. 85–87.

[43]   H.J. Weyer, I. Müller, B. Schmitt, D. Bosbach, A. Putnis, Time-resolved monitoring of cement hydration: Influence of cellulose ethers on hydration kinetics, Nucl. Instruments Methods Phys. Res. Sect. B Beam Interact. with Mater. Atoms. 238 (2005) 102–106. doi:10.1016/j.nimb.2005.06.026.

[44]   J. Pourchez, P. Grosseau, R. Guyonnet, B. Ruot, HEC influence on cement hydration measured by conductometry, Cem. Concr. Res. 36 (2006) 1777–1780. doi:10.1016/j.cemconres.2006.06.002.

[45]   J. Pourchez, P. Grosseau, B. Ruot, Current understanding of cellulose ethers impact on the hydration of C3A and C3A-sulphate systems, Cem. Concr. Res. 39 (2009) 664–669. doi:10.1016/j.cemconres.2009.05.009.